Practical Error Bounds for Binary Tomography

Wagner Fortes[1], Jan Sijbers[2] and Kees Joost Batenburg[1,2]

[1]Centrum Wiskunde & Informatica (CWI), Science Park 123, 1098 XG Amsterdam, The Netherlands [email: W.R.Fortes@cwi.nl; joost.batenburg@cwi.nl]

[2]iMinds-Vision Lab, University of Antwerp, Universiteitsplein 1, 2610 Wilrijk, Belgium [email: jan.sijbers@ua.ac.be]

Keywords: tomographic reconstruction, binary images, error bounds

ABSTRACT

The purpose of computed tomography (CT) is to compute an accurate approximation of a scanned object from a series of its projections. As the ground truth is typically unknown, it is not straightforward to determine the quality of such an approximation. Even if the reconstructed image corresponds almost perfectly with the observed projection data, it may still be quite different from the original object if the number of projections is small.
We have recently developed a series of mathematical error bounds that provide quantitative guarantees on the quality of the reconstruction of a homogeneous object (i.e. a binary image). As these bounds are based on idealized assumptions of the imaging model (assuming perfect, noiseless data), they have to be adjusted to be useful in practice.
In this article we show how one of these error bounds can be adapted to be useful for bounding the quality of experimental images. Our experimental results suggest that even though approximations have to be made due to noise and other errors in the data, the resulting bounds can still provide guidance on estimating the reconstruction quality.

1. INTRODUCTION

In Computed Tomography (CT), an image of a scanned object is formed by reconstructing an image of the object from a series of its projections. The image represents some physical property of the original object, usually the attenuation coefficient, which in turn is related to the compositions of the object (Herman 2010). The reconstructed image is never an exact representation of the original object, for various reasons. Firstly, the measured data itself is noisy and may contain various imaging artefacts, propagating into the reconstructed image. Secondly, the reconstruction algorithm itself may not be exact, such that even for noiseless projections it does not result in a reconstructed image that matches these projections. Finally, when using a relatively small number of projections, the reconstruction problem is inherently underdetermined. This means that many solutions may exist, each satisfying the projection data (Louis 1984). To draw quantitative conclusions about the scanned object based on the reconstructed image, it is essential to determine how well the reconstruction corresponds with the original object, which we refer to as the *accuracy* of the reconstruction. At present, there is a gap in the ability to determine reconstruction accuracy. Based on the point-spread-function of forward projection and consecutive reconstruction, resolution estimates can be derived for the reconstructed image (Crowther et al. 1970). However, such a local resolution measure does not impose any bound on the global difference between the reconstructed image and the ground truth. If a large number of projections are available, linear algebra arguments can be used to test if the pixelized reconstruction is uniquely determined by the measured data (Mueller 1998, p.27). If only a small number of projections are available, experimental validation of reconstruction accuracy, using known phantoms, is the only option.
We have recently developed a mathematical approach that enables the computation of upper bounds on the reconstruction accuracy when the original object is homogeneous, i.e. corresponding to a binary image (Batenburg *et al.* 2012). These error bounds cannot be used directly on experimental images, as they are based on the assumption of perfect, noiseless projection data. In this article we show how one of these error bounds can be adapted to be useful for bounding the quality of experimental images.

2. APPROACH

The reconstruction problem in tomography can be approximated by a system of linear equations **Wv** = **p**, where $\mathbf{v} \in \mathbf{R}^n$ denotes a vector of unknown pixel values, $\mathbf{p} \in \mathbf{R}^m$ denotes a vector containing the measured projection data and $\mathbf{W} \in \mathbf{R}^{mxn}$ denotes the discretized projection operator (Chapter 7 of Kak and Slaney 2001).

In (Batenburg *et al.* 2012), it was demonstrated that for parallel beam tomography, the norm $||\mathbf{x}||_2$ of all *binary* solutions of the system **Wv** = **p** must be the same, and it can be computed directly from the projection data. This can be seen from the fact that the sum of the projected intensities in any direction equals the sum of the image pixels. So, we can determine the sum of the pixel values based on the projection data. As $0^2 = 0$ and $1^2 = 1$, this sum is equal to the sum of *squared* pixel values for any binary image **x**, and therefore the norm of all binary solutions is identical. In fact, it was shown in (Batenburg *et al.* 2012) that all binary solutions $\mathbf{x} \in \{0,1\}^n$ lie on a hypersphere centered in the minimum norm solution **x*** and having radius $\mathbf{R} = \text{sqrt}(||\mathbf{x}||^2 - ||\mathbf{x}^*||^2)$; see Fig. 1. Based on these observations, a methodology was derived to compute an upper bound on the difference between any two binary solutions, as well as an upper bound on the difference between a given binary image and any binary solution, all based on the computation of **x*** and **R**. The computation of the bounds depends on the hypersphere's center **x***, corresponding to the shortest real-valued solution of the tomography equations**.** If the projection data contains no noise or other errors, this solution can be computed efficiently using iterative methods, such as the Conjugate Gradient Least Squares (CGLS) algorithm (Saad 2003).

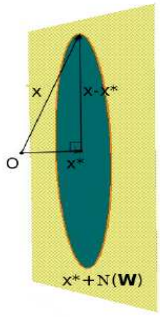

Fig. 1: *All binary solutions **x** lie on a hypersphere centered in **x****.

Now suppose that $\mathbf{b} \in \{0,1\}^n$ represents the ground truth and **p** = **Wb** represents the ideal projections of this object. In practice, the measured projection data **q** is contaminated with noise and other distortions (e.g. beam hardening, detector inefficiencies) and therefore **x*** cannot be computed, as it requires knowledge of **p**. Instead, we consider a different hypersphere containing all binary solutions of the noiseless problem. This hypersphere is centered in **z***, the minimum norm least squares solution of the available reconstruction problem **Wx**=**q**, and with radius **S** based on the theorem below, which we do not prove here:

Theorem: $\mathbf{S}^2 = ||\mathbf{z}^*||^2 - 2||\mathbf{x}^*||||\mathbf{z}^*||\cos\theta + ||\mathbf{x}||^2$.

The theorem expresses the value of **S** as a function of several terms that can be approximated based on the noisy projection data **q**. The angle θ refers to the angle between the vectors **x*** and **z***. As we cannot compute $||\mathbf{x}^*||$, $\cos\theta$ and $||\mathbf{x}||$, we approximate these three terms. We assume that the noise has a mean value of 0, such that the total summed intensity of any binary solution can still be computed approximately from the projections as $||\mathbf{q}||/k$, where *k* denotes the number of projections. Moreover, we approximate the norm $||\mathbf{x}^*||$ by $||\mathbf{z}^*||$. Finally, $\cos\theta$ was experimentally computed for several different settings yielding a value close to 1, which depends on the noise level, image size, and the general shape of the object. The radius **S** is then approximately given by

$$\mathbf{S}^2 \approx (\alpha - 1)||\mathbf{z}^*||^2 + \text{sqrt}(||\mathbf{q}||/k),$$

where α is a value close to 0 which depends on the specific problem setting and has to be calibrated based on simulation experiments using phantom images that have similar noise characteristics and similar general shape as the true object.
The computation of the bounds are the same as given in (Batenburg *et al.* 2012), but using the hypersphere centered in **z*** and radius **S** as given above.

3. EXPERIMENTS

Simulation experiments have been performed to determine if the error bounds for noiseless data can be computed based on noisy projection data. Here we present the result of one such experiment.

One of the bounds in (Batenburg *et al.* 2012) concerns an upper bound on the number of pixel differences between any binary solution of the tomography problem **Wv** = **p** and the *rounded shortest real-valued solution* **r**. The image **r** can be computed from the projection data by applying the CGLS algorithm and rounding each entry of the result to the nearest binary number. The advantage of this particular bound, is that it can be verified without knowledge of *all* binary solutions. Other bounds given in the same paper deal with the differences between any *two* binary solutions, but these bounds cannot be verified based on a single phantom image. Therefore, we focus here on the bound with respect to **r**.

Simulated projections were computed based on downsampled versions of the phantom in Fig. 2(a), using a strip model for the projection operator (Kak and Slaney 2001, Section 7.4.1) and equiangular projections. The phantom was downsampled to binary images of size 32x32 and 128x128, respectively, and all experiments were carried out at both these sizes. A moderate amount of additive Gaussian noise was then applied to the projections, yielding the vector **q**, to be used for computing the bounds.

The vector **z*** was computed using the CGLS algorithm. The parameter α was found to be dependent on image size, type of phantom, noise level and number of projections; it was set to two different values, 0 and 0.02, in our experiments. In Fig. 2(b) and 2(c), we show the relative number of pixels (as a fraction of the total number) that differ between the phantom image in Fig. 2a and the result of rounding **z*** to the nearest binary image, which is marked by the label "true error" (red curve), as a function of the number of projection angles. The estimated error bound for the two values of α are labelled by B0 (α = 0, blue curve) and B0.02 (α = 0.02, black curve). The blue curve could not be plotted for most of the angles, as the resulting squared radius $\mathbf{S}^2$ became negative. The black curve, however, can be computed for all angles and tracks the true error rather well: although the shape of the curve is somewhat irregular, the estimated error stays within an order of magnitude from the true error for all experiments.

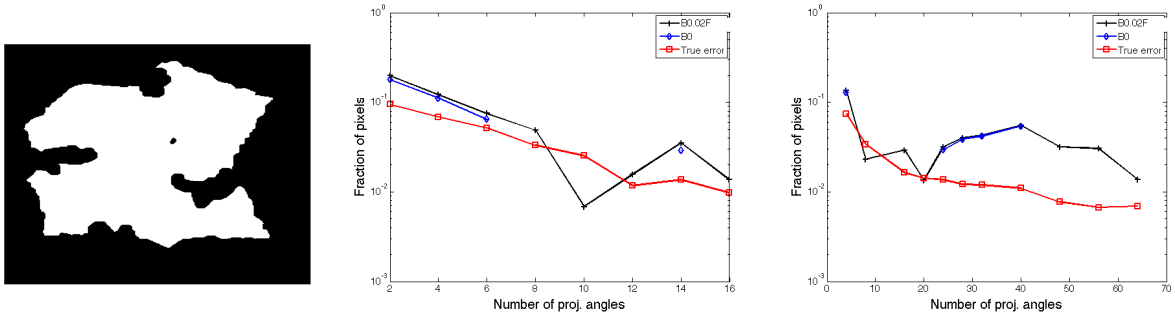

Fig 2: *(a) Binary phantom of size 512x512; (b) Computed error bounds for a downscaled phantom of size 32x32; (c) Computed error bounds for a downscaled phantom of size 128x128.*

In Fig. 3, some results are shown for an experimental micro-CT dataset of a diamond, acquired using a Scanco micro-CT 40 X-ray scanner based on 500 projections. Fig. 3(a) shows a FBP-reconstructed slice based on all 500 projections, while Fig. 3(b) and 3(c) show binary reconstructions computed by applying CGLS and rounding the result based on 10 and 20 projections, respectively. The corresponding

approximated error as a function of the number of projection angles is shown in Fig. 3(d), based on a value of α= 0.02.

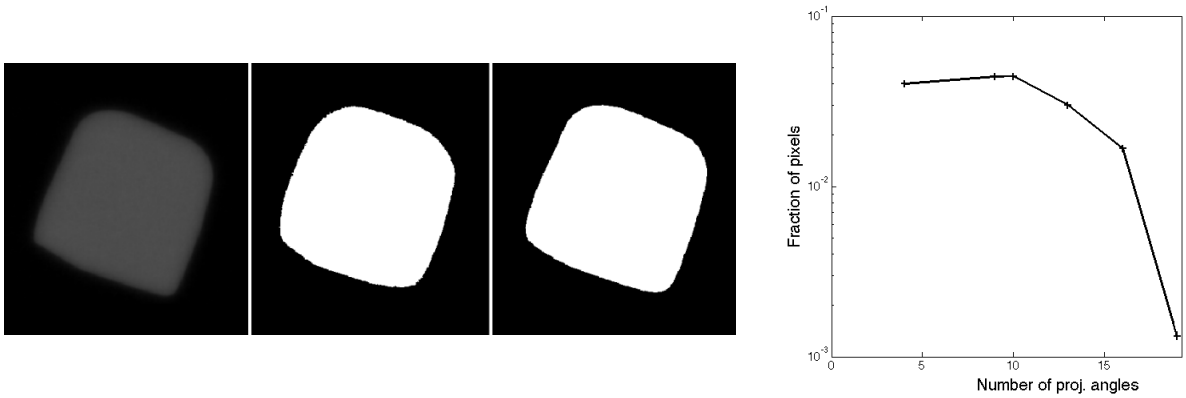

Fig 3: *(a) Slice of a diamond from an experimental micro-CT dataset; (b) Binary reconstruction from 10 projections; (c) Binary reconstruction from 20 projections; (d) Computed error bound on the difference between the binary reconstruction and the true image, as a function of number of angles.*

4. DISCUSSION & CONCLUSIONS

The approach provided here is the first technique for estimating a global image error in binary image reconstruction that can be applied to a set of noisy projections.

The experimental results demonstrate that error estimates for binary tomography can be computed based on noisy, non-ideal projection data. The computed estimates have similar properties to the theoretical estimates that can only be computed if perfect, noiseless projection data is available. Further research is needed to establish how the factor α should be chosen in various scenarios, to further validate the approach, and to scale it up to larger images.

5. ACKNOWLEDGEMENTS

K.J.B. was supported by the Netherlands Organisation for Scientific Research (NWO), programme 639.072.005. We thank Matthias Uyttendaele of DiamCad for providing the micro-CT data.

6. REFERENCES

Batenburg K.J., Fortes W., Hajdu L., and Tijdeman R. (2012) Bounds on the quality of reconstructed images in binary tomography. Discrete Applied Mathematics, to appear.

Crowther R.A., Derosier D.J., and Klug A. (1970) Reconstruction of 3-dimensional structure from projections and its application to electron microscopy, Proceedings of the Royal Society of London Series A Mathematical and Physical Sciences 317 (1530) 319-340.

Herman G.T. (2010) Fundamentals of Computerized Tomography, 2nd edition, Springer.

Kak A.C. and Slaney M. (2001) Principles of Computerized Tomographic Imaging. SIAM.

Louis A.K. (1984) Nonuniqueness in inverse radon problems: The frequency distribution of the ghosts, Mathematische Zeitschrift 185(3), 429-440.

Mueller K. (1998) Fast and accurate three-dimensional reconstruction from cone-beam projection data using algebraic methods, PhD dissertation, The Ohio State University.

Saad, Y. (2003) Iterative Methods for Sparse Linear Systems. SIAM.